

Semi-supervised Salient Object Detection with Effective Confidence Estimation

Jiawei Liu, Jing Zhang, Nick Barnes
Australian National University

{jiawei.liu3, jing.zhang, nick.barnes}@anu.edu.au

Abstract

The success of existing salient object detection models relies on a large pixel-wise labeled training dataset. However, collecting such a dataset is not only time-consuming but also very expensive. To reduce the labeling burden, we study semi-supervised salient object detection, and formulate it as an unlabeled dataset pixel-level confidence estimation problem by identifying pixels with less confident predictions. Specifically, we introduce a new latent variable model with an energy-based prior for effective latent space exploration, leading to more reliable confidence maps. With the proposed strategy, the unlabelled images can effectively participate in model training. Experimental results show that the proposed solution, using only 1/16 of the annotations from the original training dataset, achieves competitive performance compared with state-of-the-art fully supervised models.

1. Introduction

As a class-agnostic image segmentation task, salient object detection (SOD) [2, 74] aims to localise the full scope of objects that attract human attention. Most existing SOD models are fully-supervised [5, 60, 77], where a pixel-wise labeled dataset [57] is used to learn a mapping function from the input space to the output space. Within this setting, methods usually focus on effective feature aggregation [58, 63, 72, 77] to achieve structure-preserving saliency prediction [5, 60].

The success of the fully-supervised methods comes from large pixel-wise labeled training datasets [58, 63, 75, 77]. However, annotation is both time-consuming and very expensive, e.g. it takes 2-3 months and costs 10K dollars to fully annotate a 10K image training dataset. To relieve the labelling burden, some research focuses on weakly-supervised saliency detection with easy-to-obtain annotations, e.g., image level labels [30, 57], scribbles [76], etc. Semi-supervised learning [35, 73] is another interesting approach to ease the labeling burden. It can learn an effective model from a training dataset with only a small number of

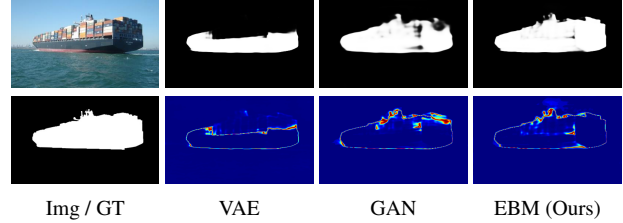


Figure 1. Pseudo-label and uncertainty map of the unlabeled training sample estimated by three generative models including VAE, GAN and EBM (Ours). The VAE generates pseudo-labels and an uncertainty map that are largely incorrect. The GAN yields an intermediate-quality pseudo label with a partially incorrect uncertainty map. Our model generates the highest-quality pseudo label with a correct uncertainty map highlighting the most errors.

labelled images. Different from weakly-supervised learning where the annotations have a different format from full annotations, in semi-supervised learning, we have access to a small set of fully annotated images, e.g. 10% of the original training dataset.

With a large unlabeled dataset, the main focus of existing semi-supervised learning methods is to effectively explore the contribution of an unlabeled set to update model parameters via self-supervised learning [61, 67, 71], pseudo label quality estimation [29, 39, 73], etc. For self-supervised learning, the unlabeled set is involved in model updating via some consistency loss functions, which constrain the model to achieve predictions that are robust to some transformations via data augmentation. For the pseudo label quality estimation approaches, the semi-supervised learning problem is usually formulated as learning from noisy labels.

In this paper, we focus on pseudo label quality estimation, and introduce the first latent variable model with an energy-based prior for pseudo label quality estimation, leading to reliable unlabeled image prediction evaluation. Three main modules are included in our framework, as shown in Fig. 2: 1) a saliency generator $g_\beta(x, z)$ to produce stochastic saliency predictions for the input image x ; 2) an energy-based prior model for effective latent space exploration that generates a reliable confidence map; 3) a confidence-aware learning strategy to encourage confident

unlabeled samples to contribute to model updating.

Different from the existing semi-supervised salient object detection techniques that are based on generative adversarial learning [55, 73] or active learning [35], we design a probabilistic approach that enables an uncertainty-based semi-supervised learning framework. The uncertainty map estimated from the prediction distribution is a reliable indicator of the gap between the pseudo label and the ground truth of unlabeled training data as shown in Fig. 1. It provides an effective solution to prevent the persistent error propagation associated with the utilisation of unlabeled training data in semi-supervised learning. Different from existing latent variable model based semi-supervised learning frameworks [19, 36], where the latent variable is assumed to follow Gaussian distribution, we model the prior of the latent variable with an energy-based model [43, 44], leading to a more informative latent space exploration and more reliable uncertainty maps. Further, we adopt a latent variable model [8] suffering no posterior collapse issue [9]. Combining it with the energy-based prior model, we observe more reliable confidence for the unlabeled samples compared with other alternative generative models, *e.g.* variational auto-encoder (VAE) [20, 53]

We summarise our main contributions as: 1) We propose the first latent variable model for the semi-supervised salient object detection task, and formulate it as a pseudo label confidence learning problem. 2) We introduce a non-Gaussian prior distribution using an energy-based model for the latent variable in semi-supervised segmentation task. The informative latent space exploration leads to more accurate confidence estimation that enables effective utilisation of the unlabeled training data. 3) Based on reliable confidence modeling, we achieve competitive performance compared with the state-of-the-art fully-supervised model with pixel-level annotations provided for only 1/16 of the training data.

2. Related Work

Salient Object Detection (SOD): Most existing SOD methods are based on deep learning models. Early approaches [31, 56, 81] adopted multi-layer perceptrons (MLPs) to predict the salient object map. They are generally outperformed by more recent fully convolutional network (FCN) based methods which leverage the more powerful representation ability of CNN. Feature aggregation [58, 63, 72, 77] and deep supervision [13, 14, 16, 78] are commonly adopted in these methods to refine prediction. There are also works exploring incorporating additional information in preserving the detailed structure of salient objects, *e.g.* object boundary [5, 60], fixation [21, 59]. Another branch of research [34, 82] uses the attention mechanism to exploit the local-global dependencies in handling the SOD task. The latest work advances the idea of attention by util-

ising a vision transformer [37].

Semi-supervised Learning: Semi-Supervised Learning (SSL) addresses the annotation shortage by incorporating a large amount of unlabeled data in training a classifier. It has been extensively studied on classification tasks with many works focusing on consistency based [23, 41, 50, 51, 54, 66] and pseudo-label based [1, 26, 61, 67, 71] techniques. Recent research has extended these approaches to semi-supervised segmentation tasks, *e.g.* semantic segmentation and medical image segmentation.

Consistency-based methods constrain the predictions of unlabeled training samples to be consistent under different perturbations [3, 22, 45]. In addition to the consistency regularisation, S4GAN [40] further utilises a discriminator on top of a typical teacher-student paradigm to filter the irrelevant classes. ATSO [15] observes a persistent error propagation issue between the teacher and student models, and proposes asynchronous optimisation as a solution. RML [79] proposes to employ two pairs of teacher-student models with heterogeneous network architectures. The mutual supervision provided by the teacher prevent direct interaction between student models, thus reducing the coupling effect. Pseudo-label based methods explore incorporating unlabeled data into training with high-quality pseudo labels. AdvCAM [27] presents an adversarial climbing technique to push the prediction away from the decision boundary. The predictions accumulated in the iterative process serve as pseudo labels of the unlabeled data. PseudoSeg [85] studies the effective combination of various augmentation techniques in generating high-quality pseudo labels.

Semi-supervised salient object detection has been under explored. SaliencyGAN [55] designs two sets of GANs: one is tasked with generating additional images for training, and the other with predicting the salient object detection mask. FC-SOD [73] proposes an adversarial-paced learning scheme that gradually upscales the contribution from the unlabeled set, according to the quality of the pseudo labels estimated by a discriminator. SAL [35] proposes an active learning strategy that initialises using a small set of labeled samples and gradually expands it to include samples where model predictions are most inaccurate.

Deep Generative Models: The two most studied generative models are the generative adversarial network (GAN) [6] and the variational auto-encoder (VAE) [20, 53]. Both have found successful applications in fully-supervised SOD tasks [28, 75]. In the semi-supervised segmentation task, a GAN is employed to realise an effective utilisation of unlabeled samples [29, 39, 55, 73]. The alternative generative models are the Energy-Based Model (EBM) [46] and Alternative Back Propagation (ABP) [8]. EBM is learnt in a latent space and relies on an expressive generator network to map the latent variable to data space. ABP alternates between inferring the latent factor and parameter update

conditioned on the observed latent factor. It has been employed to model the bias in RGB-D salient object detection datasets [74].

Uniqueness of our solution: We propose the first latent variable model with an energy-based prior for semi-supervised salient object detection, aiming to generate reliable confidence maps for pseudo label quality evaluation. Although existing pseudo-labeling techniques [29, 39, 73] aim to prevent error propagation by identifying the incorrect predictions within the pseudo labels, for the first time, we use confidence estimation via an informative latent variable (with energy-based prior) for pseudo label quality estimation. Extensive experimental results validate our solution.

3. Our Method

3.1. Setting

For semi-supervised salient object detection, we have a dataset D consisting of N_l labeled images $D^l = \{x_i^l, y_i^l\}_{i=1}^{N_l}$, and N_u unlabeled images $D^u = \{x_j^u\}_{j=1}^{N_u}$. x_i^l, y_i^l are a labeled image and its corresponding ground truth and x_j^u represents the unlabeled image. i (or j) indexes the images, and we omit the index whenever it is clear. For semi-supervised learning, we usually have $N_l \ll N_u$. We define the empirical distribution of the labeled set and the unlabeled set as $p_l(x, y)$ and $p_u(x)$ respectively. The goal of semi-supervised learning is then to learn an accurate classifier f_θ based on both $p_l(x, y)$ and $p_u(x)$.

Conventional semi-supervised learning techniques can be roughly divided into two main categories: 1) consistency regularisation via self-supervised learning strategies [3, 22, 45] and 2) pseudo label exploration [29, 39, 73] to effectively encourage unlabeled data to contribute to model updating. The proposed solution belongs to the second direction, where we aim to introduce a pseudo label quality estimation technique via a latent variable model [8] for effective semi-supervised saliency detection.

3.2. Challenges of Pseudo-Labeling

The success of consistency regularisation based semi-supervised learning methods [3, 22, 45] largely relies on the perturbation/augmentation based consistency loss - their performance is limited in the absence of rich sets of augmentations. Pseudo-Labeling [29, 39, 73] techniques do not require domain specific data augmentation, making them easier to implement. However, directly using the generated pseudo label for model updating is problematic, as serious error-propagation can lead to a biased model over-fitting to the noisy pseudo label [15]. To achieve effective pseudo-labeling based semi-supervised learning, the model should be aware of its prediction on the unlabeled set, and we should discard or decrease the contribution of noisy sam-

ples for updating the model. In this paper, we introduce a latent variable model [8] based confidence-aware learning pipeline for semi-supervised salient object detection, where randomness of the latent variable makes it possible to estimate the confidence of model prediction. Our model can effectively identify noisy samples, and prevent them from dominating the model updating.

3.3. The Proposed Framework

We show the learning pipeline of the proposed semi-supervised learning saliency detection network in Fig. 2. Following the pseudo label based semi-supervised learning pipeline, we first design a stochastic saliency generator $g_\beta(x, z)$ via a latent variable model [8] to produce a saliency prediction $g_\beta(x^l, z)$ for the labeled image x^l and $g_\beta(x^u, z)$ for the unlabeled image x^u . Our next step is evaluating the pixel-wise confidence of the unlabeled prediction (the pseudo label $g_\beta(x^u, z)$) to achieve confidence-aware semi-supervised learning.

Latent Variable Model for Confidence Estimation: Confidence estimation is used to explore model limitations with an extra confidence score (or the inverse uncertainty score) representing the over-fitting degree (or calibration degree [7, 17]) of the trained model. Existing techniques include Monte Carlo Dropout (MC-Dropout) [17] and deep ensemble [24]. The former is usually achieved via applying random dropout at both train and test time, and the latter is obtained by copying part of or the whole framework multiple times, and initializing each of them separately.

Both MC-Dropout and deep ensemble can produce multiple predictions for each input image. However, recent research [4] finds that the former usually fails to explore the true representation of the model uncertainty as random dropout may produce parameters that lie in a very compact manifold. For the latter, the performance of the final uncertainty is highly related to the design of the ensemble structure. Further, the fixed structure makes it not sufficiently flexible to generate stochastic predictions. Alternatively, we can use latent variable model [6, 8, 20] to generate stochastic predictions. Specifically, we use a random variable z to represent the uncertainty of the generated pseudo label.

Given the ‘‘stochastic attribute’’ of our saliency generator $g_\beta(x, z)$, we can sample from the posterior distribution $q_\beta(z|x^l, y^l)$ of the latent variable z to obtain stochastic predictions for the labeled set D^l . To get stochastic predictions for the unlabeled set, as no ground truth exists, we can only sample from the prior distribution $p_\alpha(z)$ of z , where α is the parameter set of the prior model. Extra regularisation is needed to constrain the similarity of the posterior and prior distribution, *e.g.* KL divergence is used in variational auto-encoder [20]. With the prior of z , the confidence of the pseudo label can be obtained as:

$$C^u = 1 - \mathbb{H}[\mathbb{E}_{p_\alpha(z)}(g_\beta(x^u, z))], \quad (1)$$

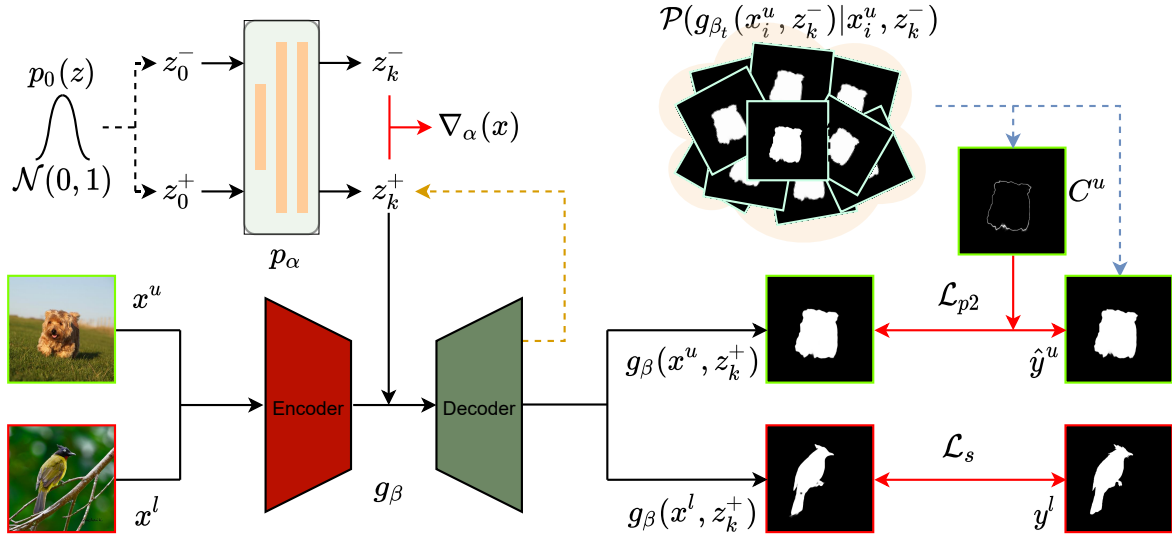


Figure 2. The probabilistic semi-supervised salient object detection network with energy-based prior model, which includes a saliency generator $g_\beta(x, z)$ and an energy-based prior model p_α . At train time, the generator takes an input image and a posterior latent variable z^+ (or prior z^- for the unlabeled images) to produce probabilistic predictions as in Eq. 2. We adopt a two-phase training: (1) Train p_α and g_β with labeled samples (red) and output intermediate model weights β and α_t , (2) Generate pseudo-labels for the unlabeled sample following Eq. 10, and compute its confidence as: $C_i^u = 1 - \mathbb{H}[\hat{y}_i^u]$. Then fine-tune the model on the unlabeled samples (green) with loss function defined in Eq. 11. Dashed lines (- -) allow only the forward propagation, but not the loss back-propagation.

where $\mathbb{H}[\cdot]$ computes entropy of the input, and C^u is the estimated confidence for the unlabeled image. In practice, we use Monte Carlo integration as an approximation of the intractable integral operation.

As shown in Eq. 1, to obtain effective confidence-aware semi-supervised salient object detection, our main focus is to design a proper prior and posterior distribution model, where the latent variable z can represent the uncertainty of the prediction. The mainstream approach is via a variational auto-encoder VAE [20] (or conditional variational auto-encoder (CVAE) [53] for our case). This presents a practical solution, where the extra inference model $q_\beta(z|x, y)$ is designed to approximate the true posterior distribution. However, the posterior collapse issue [9] within the CVAE framework limits its effectiveness in exploring the true posterior distribution of the latent space, leading to less reliable uncertainty estimation when the learned posterior distribution collapses to a point instead of a distribution.

To solve the posterior collapse issue, [8] introduces “alternating back-propagation” (ABP), where they sample directly from the true posterior distribution via a Langevin dynamics based Markov chain Monte Carlo (MCMC) [42] with no extra model involved. ABP [8] defines the prior of the latent variable z as simple standard normal distribution $p_\alpha(z) = \mathcal{N}(0, 1)$. However, with the Langevin dynamics based MCMC, the obtained posterior does not necessarily follow a Gaussian distribution. This leads to inconsistent behaviour in training and testing, as z is sampled from the

posterior (a non-Gaussian distribution) at train time, while it is sampled from $p_\alpha(z) = \mathcal{N}(0, 1)$ (a Gaussian distribution) at test time. To solve this problem, [46] introduces an energy-based prior, where the prior distribution of the latent variable is modeled via an energy-based model [25, 43, 44] relaxing the “Gaussian constraint” for the prior distribution. **Energy-Based Prior:** Inspired by [46], we propose a generative learning solution to address the semi-supervised salient object detection problem with a latent variable model, where the prior distribution $p_\alpha(z)$ of z is modeled with an energy-based model, and α represents the parameters. To avoid the possible posterior collapse issue [9], we adopt alternating back-propagation [8], where the posterior of z is sampled directly from the true posterior distribution $q_\beta(z|x, y)$ via Langevin Dynamics based MCMC [42].

For an input image x , and the latent variable z , our generative model is defined as:

$$\begin{aligned} z &\sim p_\alpha(z), \\ y &= g_\beta(x, z) + \epsilon, \end{aligned} \quad (2)$$

where $p_\alpha(z)$ is the prior of z , which is formulated as an energy-based model, and $\epsilon \sim \mathcal{N}(0, \sigma_\epsilon^2 I)$ represents the inherent observation noise, and σ_ϵ^2 represents the noise level, which is usually tuned instead of estimated. The generative learning framework enables uncertainty-based semi-supervised learning that maximises the utilisation of reliable information from unlabeled data while avoiding corruption incurred by persistent error propagation [15].

The energy-based prior distribution $p_\alpha(z)$ is defined as:

$$p_\alpha(z) = \frac{1}{Z(\alpha)} \exp(f_\alpha(z)) p_0(z) \quad (3)$$

where $f_\alpha(z)$ is the negative energy, modeled by a multi-layer perceptron (MLP) network, $p_0(z) = \mathcal{N}(0, \sigma_z^2 I)$ is a reference distribution with a tuned hyper-parameter σ_z^2 , and $Z(\alpha) = \int \exp[f_\alpha(z)] p_0(z) dz$ is a normalising constant that is intractable. Different from existing generative models [6, 8, 20, 53] that assume a simple isotropic Gaussian distribution, the latent variable in this work adopts the form of the energy-based correction [46] of an isotropic Gaussian reference distribution [65] as defined in Eq. 4:

$$p_\alpha(z) \propto \exp[f_\alpha(z) - \frac{1}{2\sigma_z^2} \|z\|^2], \quad (4)$$

where we usually define the energy function as: $\mathcal{E}_\alpha(z) = -f_\alpha(z) + \frac{1}{2\sigma_z^2} \|z\|^2$.

Cooperatively Learning of the Saliency Generator and Energy-based Prior Model: We have two main modules within our framework, namely a saliency generator $g_\beta(x, z)$ and an energy-based prior model $p_\alpha(z)$, where both β and α can be updated via maximum likelihood estimation (MLE). Denoting the parameter $\theta = \{\alpha, \beta\}$, the data log-likelihood is defined as:

$$\begin{aligned} L(\theta) &= \frac{1}{n} \sum_{i=1}^n \log p_\theta(y_i | x_i) \\ &= \frac{1}{n} \sum_{i=1}^n \log \left[\int g_\beta(y_i | x_i, z_i) p_\alpha(z_i) dz_i \right]. \end{aligned} \quad (5)$$

By computing the gradient of $L(\theta)$, we obtain gradients for both the energy-based prior model parameters α and generator parameters β as:

$$\begin{aligned} E_{p_\theta(z|x,y)}[\nabla_\alpha \log p_\alpha(z)] \\ = E_{p_\theta(z|x,y)}[\nabla_\alpha f_\alpha(z)] - E_{p_\alpha(z)}[\nabla_\alpha f_\alpha(z)]. \end{aligned} \quad (6)$$

Empirically, the energy-based prior model is updated based on the energy difference between the posterior and prior distributions of latent variable z . Similarly, the gradients of the saliency generator are:

$$\begin{aligned} E_{p_\theta(z|y,x)}[\nabla_\theta \log p_\theta(y|x, z)] \\ = E_{p_\theta(z|y,x)}[\nabla_\theta \left[\frac{1}{\sigma^2} (y - g_\beta(x, z)) \nabla_\beta g_\beta(x, z) \right]] \end{aligned} \quad (7)$$

The expectations in Eq. 6 and Eq. 7 can be approximated via Langevin Dynamics [42, 84] based MCMC sampling [33], which iterates over the sampling process based on gradients as shown in Eq. 8 and Eq. 9 for prior and posterior latent variables z^- and z^+ respectively.

$$z_{k+1}^- = z_k^- - \delta \nabla_z \mathcal{E}_\alpha(z_k^-) + \sqrt{2\delta} \epsilon_k, \quad (8)$$

$$\begin{aligned} z_{k+1}^+ &= z_k^+ + \sqrt{2\delta} \epsilon_k \\ &- \delta \left[\nabla_z \mathcal{E}_\alpha(z_k^+) - \frac{1}{\sigma_\epsilon^2} (y - g_\beta(x, z_k^+)) \nabla_z g_\beta(x, z_k^+) \right] \end{aligned} \quad (9)$$

where $p_0(z) = \mathcal{N}(0, 1)$ and $\epsilon_k \sim \mathcal{N}(0, 1)$ for both the prior and posterior distributions. δ is the step size of Langevin Dynamics, which can be set differently for prior and posterior distribution. In practice, we run $K^- = 5$ Langevin steps of the prior with step size δ^- , and $K^+ = 5$ Langevin steps of the posterior with step size δ^+ .

Confidence-aware Semi-Supervised Learning Eq. 8 and Eq. 9 provide iteration strategies for both the prior and posterior of the latent variable. In practice, we can sample from $p_0(z)$ to obtain z_0^- and z_0^+ , and obtain the updated prior z^- and posterior z^+ by running a given number of Langevin steps. Specifically, our semi-supervised learning solution consists of two phases. (1) The network is trained on labeled set D^l in a fully supervised setting with a structure-aware loss function [62], which is a combination of binary cross entropy loss and dice loss. We then define the first phase loss function as: $\mathcal{L}_{p1} = \mathcal{L}_s$, where \mathcal{L}_s is the structure-aware loss [62]. At the end of phase (1), we obtain pseudo labels \hat{y}^u for the unlabeled set as:

$$\hat{y}_i^u = \frac{1}{J} \sum_{j=1}^J g_\beta(x_i^u, z_j), z_j \sim p_\alpha(z), i = 1, \dots, N_u \quad (10)$$

where we set the total forward passes: $J = 10$. Similar to Eq. 1, the pixel-wise uncertainty (the inverse confidence) associated with the pseudo labels can be estimated by computing the entropy of mean prediction as: $u_i^u = \mathbb{H}[\hat{y}_i^u]$.

In phase (2), we train the model on the unlabeled set $D^u = \{x^u, \hat{y}^u, u^u\}$. We use a weighted structure-aware loss for the unlabeled set, where the loss function is weighed by the inverse pixel-wise uncertainty (the confidence) $C_i^u = 1 - u_i^u \in [0, 1]$. Further, an entropy loss is incorporated to prevent overly smoothed predictions as a result of using soft pseudo labels. The overall loss function in phase (2) training is then defined as:

$$\mathcal{L}_{p2} = \lambda_{us} C^u \mathcal{L}_s(g_\beta(x^u, z^-), \hat{y}^u) + \lambda_{ue} \mathbb{H}[\hat{y}^u] \quad (11)$$

where $\mathbb{H}[\hat{y}^u] = -\hat{y}^u \cdot \log(\hat{y}^u)$ is the entropy loss, and \cdot is the dot product. Empirically we set $\lambda_{us} = \lambda_{ue} = 1$.

3.4. Network Details

Saliency Generator: Our saliency generator $g_\beta(x, z)$ is a typical U-Net framework with an encoder and decoder. We built our encoder with the ResNet50 backbone, which can produce four levels of backbone features: $\{s_k\}_{k=1}^4$. We adopt the decoder of MiDaS [49], which consists of four fusion blocks ($\{F_i\}_{i=1}^4$). The first fusion block upscales the highest-level feature ($\bar{s}_4 = F_4(s_4)$) by a factor of two. The

Table 1. Performance comparison with state-of-the-art fully-/weakly-/semi-supervised SOD methods on benchmark testing dataset. P - pixel-level label; I - image-level label; C - caption; S - scribble.

Methods	Label	DUTS-TE [57]		DUT-OMRON [69]		PASCAL-S [68]		SOD [38]		ECSSD [52]		HKU-IS [31]		
		$F_{\xi}^{\max} \uparrow$	$\mathcal{M} \downarrow$											
Fully-Supervised	CPD [64]	P	0.865	0.043	0.797	0.056	0.859	0.071	0.860	0.112	0.939	0.037	0.925	0.034
	BASNet [48]	P	0.859	0.048	0.805	0.056	0.854	0.076	0.851	0.114	0.942	0.037	0.928	0.032
	PoolNet [32]	P	0.888	0.039	0.815	0.053	0.863	0.075	-	-	0.944	0.039	0.932	0.033
	EGNet [80]	P	0.888	0.039	0.815	0.053	0.865	0.074	0.889	0.099	0.947	0.037	0.935	0.031
	MINet [47]	P	0.884	0.037	0.810	0.056	0.867	0.064	-	-	0.947	0.033	0.935	0.029
	ITSD [83]	P	0.882	0.041	0.820	0.061	0.870	0.064	-	-	0.947	0.034	0.934	0.031
Weakly-Supervised	WSS [57]	I	0.740	0.099	0.695	0.110	0.773	0.140	0.778	0.171	-	-	-	-
	MWS [70]	I & C	0.768	0.091	0.722	0.108	0.786	0.134	0.801	0.170	0.878	0.096	0.856	0.084
	ASMO [30]	I	-	-	0.732	0.100	0.758	0.154	0.758	0.187	-	-	-	-
	SS [76]	S	0.789	0.062	0.753	0.068	0.811	0.092	0.806	0.131	0.888	0.061	0.880	0.047
Semi-Supervised	SaliencyGAN [55]	1,000	0.641	0.135	0.610	0.131	0.699	0.164	-	-	0.776	0.116	0.742	0.107
	SAL [35]	1,500	0.849	0.046	0.766	0.062	0.804	0.088	0.835	0.105	0.884	0.057	0.920	0.032
	FC-SOD [73]	1,000	0.846	0.045	0.767	0.067	0.848	0.067	0.846	0.122	0.914	0.047	0.903	0.038
EBM-SOD Ours	659 ($\frac{1}{16}$)	0.869	0.045	0.774	0.067	0.864	0.067	0.856	0.104	0.931	0.043	0.928	0.034	

subsequent fusion blocks gradually fuse feature pairs and upscale the resultant feature by a factor of two to produce $\{(\bar{s}_{k-1} = F_{k-1}(\bar{s}_k, s_{k-1}))\}_{k=4}^2$. The output layer adopts the final feature \bar{s}_1 and produces a binary saliency map y' of the same spatial size as the input image. With the saliency generator, we obtain a saliency prediction for the labeled set $g_{\beta}(x^l, z)$, and pseudo label $g_{\beta}(x^u, z)$ for the unlabeled set.

Energy-based prior model (p_{α}): is parameterised by a multi-layer perceptron (MLP) to model the energy function in latent space. It takes the latent variable as input and outputs an energy value. The model consists of three fully-connected layers of dimensions $\{d_z, 100, 100\}$ where d_z is the dimension of the latent variable. Each fully connected layer, except the last one, is followed by a GELU [12] activation function.

4. Experimental Results

4.1. Setup

Dataset: We train our proposed semi-supervised learning method on the DUTS [57] training dataset with six different labeled set split ratios, including 1/64, 1/32, 1/16, 1/8, 1/4 and 1/2. Our method is further evaluated on six SOD benchmark datasets, including the DUTS test set [57], DUT-OMRON [69], PASCAL-S [68], SOD [38], ECSSD [52] and HKU-IS [31]. We report our performance trained using a labeled ratio of 1/16 ($N_l = 659$) in Tab. 1.

Evaluation metrics: Following previous works [55, 73], we adopt maximum F-measure (F_{ξ}^{\max}) and mean absolute error (MAE \mathcal{M}) as our evaluation metrics.

Implementation details: 1) Training details: We implement our method in the Pytorch framework. The encoder has a ResNet-50 [10] backbone. The decoder and the energy-based model are initialised by default. Our proposed method is trained with the Adam optimiser [18]. All im-

ages are rescaled to 480×480 in resolution. For both phase (1) and phase (2) training, the learning rates of the generator model and the energy-based model are initialised to $l_G = 2.5 \times 10^{-5}$ and $l_E = 1 \times 10^{-5}$ respectively. The learning rates are decayed by a factor of 0.9 after every 1,000 iterations. With a fixed batch size of 8, the training is composed of 6,500 iterations in phase (1) and 8,500 iterations in phase (2). The complete training takes 7 hours using a single NVIDIA Geforce RTX 3090 GPU.

2) Semi-supervised model related hyper-parameters: In our experiment, we run $K^- = K^+ = 5$ Langevin steps with step size $\delta^- = 0.4$ and $\delta^+ = 0.1$ for the prior and posterior model respectively. Empirically, we set the hyper-parameter $\sigma_z^2 = 1.0$ and $\sigma_{\epsilon}^2 = 0.3$.

4.2. Performance Comparison

As there are few semi-supervised salient object detection models, we also include fully-supervised and weakly-supervised SOD models for comparison on benchmark datasets in Tab. 1.

Quantitative comparison: It can be seen in Tab. 1 that our proposed method performs favourably against previous state-of-the-art semi-supervised SOD methods on all six datasets. It is worth noting that we achieve these performances using only 659 fully labeled images, which is much less compared to 1,000 required by SaliencyGAN [55] and FC-SOD [73] and 1,500 by SAL [35]. We significantly outperform FC-SOD and SAL in terms of the F-max measure on the DUTS, PASCAL-S, ECSSD and HKU-IS datasets. Further, we use a smaller ResNet-50 backbone compared to the ResNet-101 of FC-SOD. Our \mathcal{M} evaluations are comparable to SAL. This can be attributed to the fact that we use far fewer pixel-level labels, resulting in over-smoothed, though correct, predictions.

Our proposed method outperforms the SOD methods

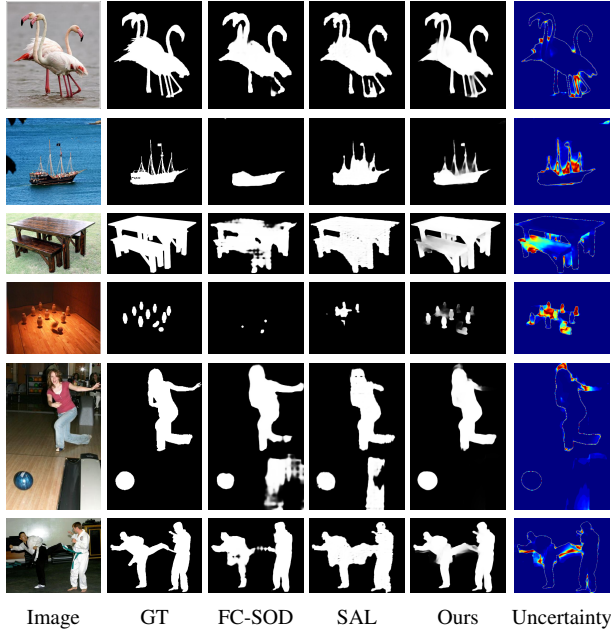


Figure 3. Predictions of our method and those compared semi-supervised SOD methods.

trained with weak annotations including image-level labels, scribbles and captions. We are significantly ahead of SS [76], the best performing weakly-supervised SOD method, which incorporates foreground and background scribbles as supervision for all training images. Compared to fully-supervised SOD methods, our approach achieves similar performance on the PASCAL-S and HKU-IS datasets. Our method can even outperform fully-supervised methods CPD [64] and BASNet [48] on DUTS and PASCAL-S datasets while using only 659 fully labeled training images.

Qualitative comparison: In Fig. 3, we compare the SOD predictions of our method against those of the existing semi-supervised SOD methods. It can be observed that FC-SOD [73] often misses the target object partially or even entirely (row 5). On the other hand, SAL [35] tends to make bulky predictions. They are less likely to miss the salient object, compared to FC-SOD, however, the fine details around the structure boundary are lost. Our method is more accurate in locating the target object, avoiding severe under- or over-segmentation. Moreover, the predictions of our model retain the structural details of complicated objects, e.g., the masts of the boat (row 3), the mirror of the motorcycle (row 2), the legs of the cranes (row 1), the boundaries of the bench (row 4), etc. Our method also presents the uncertainties associated with its predictions. They clearly indicate the complex area where predictions are prone to mistakes. Surprisingly, the uncertainty map of the last row even captures the shadow of the arm and the leg, which are difficult to distinguish. Samples in rows 2 and 4 also present the cause

of reduced improvements in MAE than in the F-max measure. As our model is trained with only 659 labeled samples and soft pseudo labels on unlabeled samples, it tends to make over-smoothed predictions, although these pixels can be correctly recalled.

Model size and running time comparison: Our generator model consists of 90.8M parameters and the EBM model introduces a negligible 13.5K parameters. The inference speed of our method is 39.18 images per second. It is slightly slower than FC-SOD [73] which is capable of processing 44.34 images per second. This slight difference can be attributed to the Langevin dynamics steps required to update the prior latent variable.

4.3. Ablation Study

These experiments investigate the contribution of each component of our framework.

The base model performance: We evaluate the baseline performance on the 1/16 data split ratio. The model trained with only labeled data is denoted as the “Base”. “Full” represents our model of training with both labeled and unlabeled sets. We conduct the experiments with five randomly labeled set splits and report and mean and standard deviation of the performances in this comparison. It can be observed in Tab. 2 that the “Base” model is sensitive to the initial selection of the labeled data. Its standard deviation is larger on the more difficult testing datasets. After finetuning the “Base” model on the unlabeled set with pseudo labels, the standard deviations are reduced on all testing datasets. Furthermore, the “Full” model consistently outperforms the “Base” model on F_{ξ}^{\max} measure with a non-overlapping standard deviation range with the “Base” model. More detailed results are provided in the supplementary material.

Latent variable without EBM prior: We conduct an experiment to study the effectiveness of the energy-based model based on the “Full” model in Tab. 2. More specifically, we train the “Full” model without the Langevin dynamics update on the prior latent variable for both phases, denoted as “NP”. In this case, the prior latent variable is directly sampled from the Gaussian distribution for both training and inference. Tab. 2 shows its deteriorated performance compared with the “Full” model.

Table 2. Model performance (F_{ξ}^{\max}) w.r.t. the usage of unlabeled set (“Base” vs “Full”) and the prior distribution (“NP” vs “Full”).

Model	DUTS-TE [57]	DUT-OMRON [69]	PASCAL-S [68]
Base	0.840 ± 0.011	0.748 ± 0.006	0.846 ± 0.006
NP	0.861 ± 0.006	0.764 ± 0.005	0.861 ± 0.005
Full	0.869 ± 0.004	0.774 ± 0.005	0.864 ± 0.004
Model	SOD [38]	ECSSD [52]	HKU-IS [31]
Base	0.840 ± 0.007	0.919 ± 0.004	0.915 ± 0.003
NP	0.849 ± 0.006	0.926 ± 0.002	0.924 ± 0.001
Full	0.856 ± 0.004	0.931 ± 0.001	0.928 ± 0.001

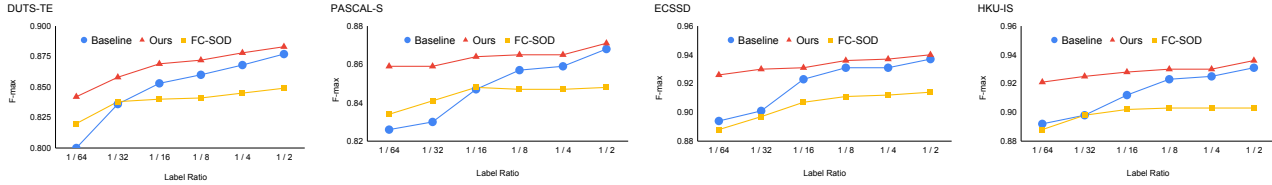


Figure 4. Comparisons of baseline, our model and FC-SOD trained on dataset splits including 1/64, 1/32, 1/16, 1/8, 1/4 and 1/2 on the four benchmark testing datasets. Results on DUT-OMRON and SOD datasets are provided in the supplementary materials.

Vary the labeled set (both the size and the samples):

Fig. 4 compares the baseline, FC-SOD and our model trained with six data splits including 1/64, 1/32, 1/16, 1/8, 1/4 and 1/2 using the F-max measure. The baseline model trained with only labeled data has limited performance in low data regimes, *e.g.* 1/64 and 1/32. This can be attributed to the labeled training data being insufficient for both the generator model and the EBM prior model to converge. Though FC-SOD outperforms the baseline when labeled data is scarce, it has limited performance gain in high data regimes. After further training on the unlabeled set with pseudo labels, our model consistently improves over the baseline and outperforms FC-SOD with all six data splits. Significant improvements are found in lower data regimes. Our model trained with 1/64 of the labeled data even outperforms FC-SOD trained with 1/2 on DUTS-TE, PASCAL-S, ECSSD and HKU-IS. As the ratio of labeled samples increases, the gap between our model and the baseline narrows. This is in accordance with results in semi-supervised semantic segmentation [11].

4.4. Discussion

Alternative deterministic semi-supervised solutions:

The II Model [51] and the Mean Teacher (MT) [54] are two important semi-supervised learning techniques. We reimplement them with our generator model for the semi-supervised SOD task. The “II Model*” enforces consistent predictions under different data augmentations, *e.g.* scaling, flipping and rotation. The performance of these models trained with the 1/16 data split ratio are presented in Tab. 3. Here, “Base*” model is a saliency prediction network similar to our Saliency Generator g_β without the latent variable and energy-based model. Full implementation details are provided in the supplementary materials. “II Model*” does not show much improvement over the “Base*” model. “MT*” is a more sophisticated semi-supervised learning model for classification. The results show its efficacy in semi-supervised SOD, achieving consistent improvements over the “Base*” model. However, our model still outperforms “MT*” on all testing datasets by a large margin.

Alternative generative model based semi-supervised solutions:

Alternative semi-supervised salient object de-

Table 3. Performance comparison between our model and the alternative deterministic and generative model based semi-supervised solutions on the benchmark testing datasets. * indicates our re-implementation.

Model	DUTS-TE	DUT-OMRON	PASCAL-S	SOD	ECSSD	HKU-IS
Base*	0.840	0.748	0.850	0.829	0.917	0.911
II Model*	0.831	0.747	0.844	0.833	0.915	0.915
MT*	0.853	0.760	0.857	0.841	0.925	0.922
GAN*	0.852	0.761	0.855	0.836	0.925	0.920
VAE*	0.849	0.751	0.851	0.832	0.921	0.917
Ours	0.869	0.774	0.864	0.856	0.931	0.928

tection solutions with generative models, including GAN (“GAN*”) and VAE (“VAE*”), are presented in Tab. 3. Detailed implementation is included in the supplementary materials. It can be seen that both “GAN*” and “VAE*” outperforms the “Base*” model that only utilises the labeled set. However, there still remains a large performance gap between alternative generative solutions and “Ours”. This can be attributed to the less effective latent space representation of GANs and VAEs. For the former, the latent variable is assumed to follow the less informative $\mathcal{N}(0, 1)$, and for the latter, the possible posterior collapse issue [9] leads to unreliable confidence estimation.

5. Conclusion

We introduce the first latent variable model with energy-based prior for semi-supervised salient object detection. The latent variables modeled with the energy-based model follow a non-Gaussian distribution, leading to more informative latent space exploration. We use Langevin dynamics based MCMC to update both prior and posterior latent variables to ensure consistent performance in both training and testing. The stochastic attribute of our solution enables generation of high-quality pseudo labels and accurate confidence maps from the prediction distribution of unlabeled training data. These enable a confidence-aware semi-supervised learning framework that efficiently addresses the potential error propagation issue in the utilisation of unlabeled data.

References

- [1] Avrim Blum and Tom Mitchell. Combining labeled and unlabeled data with co-training. In *Proceedings of the eleventh annual conference on Computational learning theory*, pages 92–100, 1998. 2
- [2] Ali Borji, Ming-Ming Cheng, Huaizu Jiang, and Jia Li. Salient object detection: A benchmark. *IEEE Transactions on Image Processing (TIP)*, 24(12):5706–5722, 2015.
- [3] Xiaokang Chen, Yuhui Yuan, Gang Zeng, and Jingdong Wang. Semi-supervised semantic segmentation with cross pseudo supervision. In *IEEE Conference on Computer Vision and Pattern Recognition (CVPR)*, pages 2613–2622, 2021. 2, 3
- [4] Nikita Durasov, Timur Bagautdinov, Pierre Baque, and Pascal Fua. Masksembles for uncertainty estimation. In *IEEE Conference on Computer Vision and Pattern Recognition (CVPR)*, pages 13539–13548, 2021. 3
- [5] Mengyang Feng, Huchuan Lu, and Errui Ding. Attentive feedback network for boundary-aware salient object detection. In *IEEE Conference on Computer Vision and Pattern Recognition (CVPR)*, pages 1623–1632, 2019. 1, 2
- [6] Ian Goodfellow, Jean Pouget-Abadie, Mehdi Mirza, Bing Xu, David Warde-Farley, Sherjil Ozair, Aaron Courville, and Yoshua Bengio. Generative adversarial nets. In *Conference on Neural Information Processing Systems (NeurIPS)*, volume 27, 2014. 2, 3, 5
- [7] Chuan Guo, Geoff Pleiss, Yu Sun, and Kilian Q Weinberger. On calibration of modern neural networks. In *International Conference on Machine Learning (ICML)*, pages 1321–1330, 2017. 3
- [8] Tian Han, Yang Lu, Song-Chun Zhu, and Ying Nian Wu. Alternating back-propagation for generator network. In *AAAI Conference on Artificial Intelligence (AAAI)*, 2017. 2, 3, 4, 5
- [9] Junxian He, Daniel Spokoyny, Graham Neubig, and Taylor Berg-Kirkpatrick. Lagging inference networks and posterior collapse in variational autoencoders. In *International Conference on Learning Representations (ICLR)*, 2019. 2, 4, 8
- [10] Kaiming He, Xiangyu Zhang, Shaoqing Ren, and Jian Sun. Deep residual learning for image recognition. In *IEEE Conference on Computer Vision and Pattern Recognition (CVPR)*, pages 770–778, 2016. 6
- [11] Ruifei He, Jihan Yang, and Xiaojuan Qi. Re-distributing biased pseudo labels for semi-supervised semantic segmentation: A baseline investigation. In *IEEE Conference on Computer Vision and Pattern Recognition (CVPR)*, pages 6930–6940, 2021. 8
- [12] Dan Hendrycks and Kevin Gimpel. Gaussian error linear units (gelus). *arXiv preprint arXiv:1606.08415*, 2016. 6
- [13] Qibin Hou, Ming-Ming Cheng, Xiaowei Hu, Ali Borji, Zhuowen Tu, and Philip HS Torr. Deeply supervised salient object detection with short connections. In *IEEE Conference on Computer Vision and Pattern Recognition (CVPR)*, pages 3203–3212, 2017. 2
- [14] Xiaowei Hu, Lei Zhu, Jing Qin, Chi-Wing Fu, and Pheng-Ann Heng. Recurrently aggregating deep features for salient object detection. In *AAAI Conference on Artificial Intelligence (AAAI)*, 2018. 2
- [15] Xinyue Huo, Lingxi Xie, Jianzhong He, Zijie Yang, Wengang Zhou, Houqiang Li, and Qi Tian. Atso: Asynchronous teacher-student optimization for semi-supervised image segmentation. In *IEEE Conference on Computer Vision and Pattern Recognition (CVPR)*, pages 1235–1244, 2021. 2, 3, 4
- [16] Md Amirul Islam, Mahmoud Kalash, and Neil DB Bruce. Revisiting salient object detection: Simultaneous detection, ranking, and subitizing of multiple salient objects. In *IEEE Conference on Computer Vision and Pattern Recognition (CVPR)*, pages 7142–7150, 2018. 2
- [17] Alex Kendall and Yarin Gal. What uncertainties do we need in bayesian deep learning for computer vision? In *Conference on Neural Information Processing Systems (NeurIPS)*, volume 30, pages 5574–5584, 2017. 3
- [18] Diederik P Kingma and Jimmy Ba. Adam: A method for stochastic optimization. *arXiv preprint arXiv:1412.6980*, 2014. 6
- [19] Diederik P Kingma, Shakir Mohamed, Danilo Jimenez Rezende, and Max Welling. Semi-supervised learning with deep generative models. In *Conference on Neural Information Processing Systems (NeurIPS)*, pages 3581–3589, 2014. 2
- [20] Diederik P Kingma and Max Welling. Auto-encoding variational bayes. *arXiv preprint arXiv:1312.6114*, 2013. 2, 3, 4, 5
- [21] Srinivas SS Kruthiventi, Vennela Gudisa, Jaley H Dholakiya, and R Venkatesh Babu. Saliency unified: A deep architecture for simultaneous eye fixation prediction and salient object segmentation. In *IEEE Conference on Computer Vision and Pattern Recognition (CVPR)*, pages 5781–5790, 2016. 2
- [22] Xin Lai, Zhuotao Tian, Li Jiang, Shu Liu, Hengshuang Zhao, Liwei Wang, and Jiaya Jia. Semi-supervised semantic segmentation with directional context-aware consistency. In *IEEE Conference on Computer Vision and Pattern Recognition (CVPR)*, pages 1205–1214, 2021. 2, 3
- [23] Samuli Laine and Timo Aila. Temporal ensembling for semi-supervised learning. *arXiv preprint arXiv:1610.02242*, 2016. 2
- [24] Balaji Lakshminarayanan, Alexander Pritzel, and Charles Blundell. Simple and scalable predictive uncertainty estimation using deep ensembles. In *Conference on Neural Information Processing Systems (NeurIPS)*, volume 30, 2017. 3
- [25] Yann LeCun, Sumit Chopra, Raia Hadsell, M Ranzato, and F Huang. A tutorial on energy-based learning. *Predicting structured data*, 1(0), 2006. 4
- [26] Dong-Hyun Lee et al. Pseudo-label: The simple and efficient semi-supervised learning method for deep neural networks. In *International Conference on Machine Learning (ICML) Workshop*, page 896, 2013. 2
- [27] Jungbeom Lee, Eunji Kim, and Sungroh Yoon. Anti-adversarially manipulated attributions for weakly and semi-supervised semantic segmentation. In *IEEE Conference on Computer Vision and Pattern Recognition (CVPR)*, pages 4071–4080, 2021. 2
- [28] Bo Li, Zhengxing Sun, and Yuqi Guo. Supervae: Superpixelwise variational autoencoder for salient object detection.

- In *AAAI Conference on Artificial Intelligence (AAAI)*, pages 8569–8576, 2019. [2](#)
- [29] Daiqing Li, Junlin Yang, Karsten Kreis, Antonio Torralba, and Sanja Fidler. Semantic segmentation with generative models: Semi-supervised learning and strong out-of-domain generalization. In *IEEE Conference on Computer Vision and Pattern Recognition (CVPR)*, pages 8300–8311, 2021. [1](#), [2](#), [3](#)
- [30] Guanbin Li, Yuan Xie, and Liang Lin. Weakly supervised salient object detection using image labels. In *AAAI Conference on Artificial Intelligence (AAAI)*, 2018. [1](#), [6](#)
- [31] Guanbin Li and Yizhou Yu. Visual saliency based on multi-scale deep features. In *IEEE Conference on Computer Vision and Pattern Recognition (CVPR)*, pages 5455–5463, 2015. [2](#), [6](#), [7](#), [15](#)
- [32] Jiang-Jiang Liu, Qibin Hou, Ming-Ming Cheng, Jiashi Feng, and Jianmin Jiang. A simple pooling-based design for real-time salient object detection. In *IEEE Conference on Computer Vision and Pattern Recognition (CVPR)*, pages 3917–3926, 2019. [6](#)
- [33] Jun S Liu and Jun S Liu. *Monte Carlo strategies in scientific computing*, volume 10. Springer, 2001. [5](#)
- [34] Nian Liu, Junwei Han, and Ming-Hsuan Yang. Picanet: Learning pixel-wise contextual attention for saliency detection. In *IEEE Conference on Computer Vision and Pattern Recognition (CVPR)*, pages 3089–3098, 2018. [2](#)
- [35] Yunqiu Lv, Bowen Liu, Jing Zhang, Yuchao Dai, Aixuan Li, and Tong Zhang. Semi-supervised active salient object detection. *Pattern Recognition (PR)*, 123:108364, 2021. [1](#), [2](#), [6](#), [7](#)
- [36] Lars Maaløe, Casper Kaae Sønderby, Søren Kaae Sønderby, and Ole Winther. Auxiliary deep generative models. In *International Conference on Machine Learning (ICML)*, pages 1445–1453, 2016. [2](#)
- [37] Yuxin Mao, Jing Zhang, Zhexiong Wan, Yuchao Dai, Aixuan Li, Yunqiu Lv, Xinyu Tian, Deng-Ping Fan, and Nick Barnes. Transformer transforms salient object detection and camouflaged object detection. *arXiv preprint arXiv:2104.10127*, 2021. [2](#)
- [38] David Martin, Charless Fowlkes, Doron Tal, and Jitendra Malik. A database of human segmented natural images and its application to evaluating segmentation algorithms and measuring ecological statistics. In *IEEE International Conference on Computer Vision (ICCV)*, volume 2, pages 416–423, 2001. [6](#), [7](#), [13](#), [15](#)
- [39] Robert Mendel, Luis Antonio De Souza, David Rauber, João Paulo Papa, and Christoph Palm. Semi-supervised segmentation based on error-correcting supervision. In *European Conference on Computer Vision (ECCV)*, pages 141–157, 2020. [1](#), [2](#), [3](#)
- [40] Sudhanshu Mittal, Maxim Tatarchenko, and Thomas Brox. Semi-supervised semantic segmentation with high-and low-level consistency. *IEEE Transactions on Pattern Analysis and Machine Intelligence (TPAMI)*, 43(4):1369–1379, 2021. [2](#)
- [41] Takeru Miyato, Shin-ichi Maeda, Masanori Koyama, and Shin Ishii. Virtual adversarial training: a regularization method for supervised and semi-supervised learning. *IEEE Transactions on Pattern Analysis and Machine Intelligence (TPAMI)*, 41(8):1979–1993, 2018. [2](#)
- [42] Radford M Neal et al. Mcmc using hamiltonian dynamics. *Handbook of markov chain monte carlo*, 2(11):2, 2011. [4](#), [5](#)
- [43] Erik Nijkamp, Mitch Hill, Song-Chun Zhu, and Ying Nian Wu. Learning non-convergent non-persistent short-run mcmc toward energy-based model. In *Conference on Neural Information Processing Systems (NeurIPS)*, pages 5232–5242, 2019. [2](#), [4](#)
- [44] Erik Nijkamp, Bo Pang, Tian Han, Linqi Zhou, Song-Chun Zhu, and Ying Nian Wu. Learning multi-layer latent variable model via variational optimization of short run mcmc for approximate inference. In *European Conference on Computer Vision (ECCV)*, pages 361–378. Springer, 2020. [2](#), [4](#)
- [45] Yassine Ouali, Céline Hudelot, and Myriam Tami. Semi-supervised semantic segmentation with cross-consistency training. In *IEEE Conference on Computer Vision and Pattern Recognition (CVPR)*, pages 12674–12684, 2020. [2](#), [3](#)
- [46] Bo Pang, Tian Han, Erik Nijkamp, Song-Chun Zhu, and Ying Nian Wu. Learning latent space energy-based prior model. In *Conference on Neural Information Processing Systems (NeurIPS)*, volume 33, 2020. [2](#), [4](#), [5](#)
- [47] Youwei Pang, Xiaoqi Zhao, Lihe Zhang, and Huchuan Lu. Multi-scale interactive network for salient object detection. In *IEEE Conference on Computer Vision and Pattern Recognition (CVPR)*, pages 9413–9422, 2020. [6](#)
- [48] Xuebin Qin, Zichen Zhang, Chenyang Huang, Chao Gao, Masood Dehghan, and Martin Jagersand. Basnet: Boundary-aware salient object detection. In *IEEE Conference on Computer Vision and Pattern Recognition (CVPR)*, pages 7479–7489, 2019. [6](#), [7](#)
- [49] René Ranftl, Katrin Lasinger, David Hafner, Konrad Schindler, and Vladlen Koltun. Towards robust monocular depth estimation: Mixing datasets for zero-shot cross-dataset transfer. *IEEE Transactions on Pattern Analysis and Machine Intelligence (TPAMI)*, 2020. [5](#), [13](#), [14](#)
- [50] Antti Rasmus, Mathias Berglund, Mikko Honkala, Harri Valpola, and Tapani Raiko. Semi-supervised learning with ladder networks. In *Conference on Neural Information Processing Systems (NeurIPS)*, volume 28, pages 3546–3554, 2015. [2](#)
- [51] Mehdi Sajjadi, Mehran Javanmardi, and Tolga Tasdizen. Regularization with stochastic transformations and perturbations for deep semi-supervised learning. In *Conference on Neural Information Processing Systems (NeurIPS)*, volume 29, pages 1163–1171, 2016. [2](#), [8](#), [13](#)
- [52] Jianping Shi, Qiong Yan, Li Xu, and Jiaya Jia. Hierarchical image saliency detection on extended cssd. *IEEE Transactions on Pattern Analysis and Machine Intelligence (TPAMI)*, 38(4):717–729, 2015. [6](#), [7](#), [15](#)
- [53] Kihyuk Sohn, Honglak Lee, and Xinchen Yan. Learning structured output representation using deep conditional generative models. In *Conference on Neural Information Processing Systems (NeurIPS)*, volume 28, pages 3483–3491, 2015. [2](#), [4](#), [5](#), [14](#)

- [54] Antti Tarvainen and Harri Valpola. Mean teachers are better role models: Weight-averaged consistency targets improve semi-supervised deep learning results. In *Conference on Neural Information Processing Systems (NeurIPS)*, pages 1195–1204, 2017. 2, 8, 13
- [55] Chengjia Wang, Shizhou Dong, Xiaofeng Zhao, Giorgos Papanastasiou, Heye Zhang, and Guang Yang. Saliencygan: Deep learning semisupervised salient object detection in the fog of iot. *IEEE Transactions on Industrial Informatics*, 16(4):2667–2676, 2019. 2, 6
- [56] Lijun Wang, Huchuan Lu, Xiang Ruan, and Ming-Hsuan Yang. Deep networks for saliency detection via local estimation and global search. In *IEEE Conference on Computer Vision and Pattern Recognition (CVPR)*, pages 3183–3192, 2015. 2
- [57] Lijun Wang, Huchuan Lu, Yifan Wang, Mengyang Feng, Dong Wang, Baocai Yin, and Xiang Ruan. Learning to detect salient objects with image-level supervision. In *IEEE Conference on Computer Vision and Pattern Recognition (CVPR)*, pages 136–145, 2017. 1, 6, 7, 15
- [58] Tiantian Wang, Lihe Zhang, Shuo Wang, Huchuan Lu, Gang Yang, Xiang Ruan, and Ali Borji. Detect globally, refine locally: A novel approach to saliency detection. In *IEEE Conference on Computer Vision and Pattern Recognition (CVPR)*, pages 3127–3135, 2018. 1, 2
- [59] Wenguan Wang, Jianbing Shen, Xingping Dong, and Ali Borji. Salient object detection driven by fixation prediction. In *IEEE Conference on Computer Vision and Pattern Recognition (CVPR)*, pages 1711–1720, 2018. 2
- [60] Wenguan Wang, Shuyang Zhao, Jianbing Shen, Steven CH Hoi, and Ali Borji. Salient object detection with pyramid attention and salient edges. In *IEEE Conference on Computer Vision and Pattern Recognition (CVPR)*, pages 1448–1457, 2019. 1, 2
- [61] Xiao Wang, Daisuke Kihara, Jiebo Luo, and Guo-Jun Qi. Enaet: A self-trained framework for semi-supervised and supervised learning with ensemble transformations. *IEEE Transactions on Image Processing (TIP)*, 30:1639–1647, 2021. 1, 2
- [62] Jun Wei, Shuhui Wang, and Qingming Huang. F³net: Fusion, feedback and focus for salient object detection. In *AAAI Conference on Artificial Intelligence (AAAI)*, pages 12321–12328, 2020. 5
- [63] Runmin Wu, Mengyang Feng, Wenlong Guan, Dong Wang, Huchuan Lu, and Errui Ding. A mutual learning method for salient object detection with intertwined multi-supervision. In *IEEE Conference on Computer Vision and Pattern Recognition (CVPR)*, pages 8150–8159, 2019. 1, 2
- [64] Zhe Wu, Li Su, and Qingming Huang. Cascaded partial decoder for fast and accurate salient object detection. In *IEEE Conference on Computer Vision and Pattern Recognition (CVPR)*, pages 3907–3916, 2019. 6, 7
- [65] Jianwen Xie, Yang Lu, Song-Chun Zhu, and Yingnian Wu. A theory of generative convnet. In *International Conference on Machine Learning (ICML)*, pages 2635–2644, 2016. 5
- [66] Qizhe Xie, Zihang Dai, Eduard Hovy, Thang Luong, and Quoc Le. Unsupervised data augmentation for consistency training. In *Conference on Neural Information Processing Systems (NeurIPS)*, volume 33, 2020. 2
- [67] Qizhe Xie, Minh-Thang Luong, Eduard Hovy, and Quoc V Le. Self-training with noisy student improves imagenet classification. In *IEEE Conference on Computer Vision and Pattern Recognition (CVPR)*, pages 10687–10698, 2020. 1, 2
- [68] Qiong Yan, Li Xu, Jianping Shi, and Jiaya Jia. Hierarchical saliency detection. In *IEEE Conference on Computer Vision and Pattern Recognition (CVPR)*, pages 1155–1162, 2013. 6, 7, 15
- [69] Chuan Yang, Lihe Zhang, Huchuan Lu, Xiang Ruan, and Ming-Hsuan Yang. Saliency detection via graph-based manifold ranking. In *IEEE Conference on Computer Vision and Pattern Recognition (CVPR)*, pages 3166–3173. IEEE, 2013. 6, 7, 13, 15
- [70] Yu Zeng, Yunzhi Zhuge, Huchuan Lu, Lihe Zhang, Mingyang Qian, and Yizhou Yu. Multi-source weak supervision for saliency detection. In *IEEE Conference on Computer Vision and Pattern Recognition (CVPR)*, pages 6074–6083, 2019. 6
- [71] Xiaohua Zhai, Avital Oliver, Alexander Kolesnikov, and Lucas Beyer. S4l: Self-supervised semi-supervised learning. In *IEEE International Conference on Computer Vision (ICCV)*, pages 1476–1485, 2019. 1, 2
- [72] Dingwen Zhang, Junwei Han, and Yu Zhang. Supervision by fusion: Towards unsupervised learning of deep salient object detector. In *IEEE International Conference on Computer Vision (ICCV)*, pages 4048–4056, 2017. 1, 2
- [73] Dingwen Zhang, Haibin Tian, and Jungong Han. Few-cost salient object detection with adversarial-paced learning. In *Conference on Neural Information Processing Systems (NeurIPS)*, volume 33, pages 12236–12247, 2020. 1, 2, 3, 6, 7, 13
- [74] Jing Zhang, Deng-Ping Fan, Yuchao Dai, Saeed Anwar, Fatemeh Saleh, Sadegh Aliakbarian, and Nick Barnes. Uncertainty inspired rgb-d saliency detection. *IEEE Transactions on Pattern Analysis and Machine Intelligence (TPAMI)*, 2021. 1, 3
- [75] Jing Zhang, Deng-Ping Fan, Yuchao Dai, Saeed Anwar, Fatemeh Sadat Saleh, Tong Zhang, and Nick Barnes. Uc-net: Uncertainty inspired rgb-d saliency detection via conditional variational autoencoders. In *IEEE Conference on Computer Vision and Pattern Recognition (CVPR)*, pages 8582–8591, 2020. 1, 2
- [76] Jing Zhang, Xin Yu, Aixuan Li, Peipei Song, Bowen Liu, and Yuchao Dai. Weakly-supervised salient object detection via scribble annotations. In *IEEE Conference on Computer Vision and Pattern Recognition (CVPR)*, pages 12546–12555, 2020. 1, 6, 7
- [77] Lu Zhang, Ju Dai, Huchuan Lu, You He, and Gang Wang. A bi-directional message passing model for salient object detection. In *IEEE Conference on Computer Vision and Pattern Recognition (CVPR)*, pages 1741–1750, 2018. 1, 2
- [78] Pingping Zhang, Dong Wang, Huchuan Lu, Hongyu Wang, and Xiang Ruan. Amulet: Aggregating multi-level convolutional features for salient object detection. In *IEEE International Conference on Computer Vision (ICCV)*, pages 202–211, 2017. 2

- [79] Pan Zhang, Bo Zhang, Ting Zhang, Dong Chen, and Fang Wen. Robust mutual learning for semi-supervised semantic segmentation. *arXiv preprint arXiv:2106.00609*, 2021. [2](#)
- [80] Jia-Xing Zhao, Jiang-Jiang Liu, Deng-Ping Fan, Yang Cao, Jufeng Yang, and Ming-Ming Cheng. Egnnet: Edge guidance network for salient object detection. In *IEEE Conference on Computer Vision and Pattern Recognition (CVPR)*, pages 8779–8788, 2019. [6](#)
- [81] Rui Zhao, Wanli Ouyang, Hongsheng Li, and Xiaogang Wang. Saliency detection by multi-context deep learning. In *IEEE Conference on Computer Vision and Pattern Recognition (CVPR)*, pages 1265–1274, 2015. [2](#)
- [82] Ting Zhao and Xiangqian Wu. Pyramid feature attention network for saliency detection. In *IEEE Conference on Computer Vision and Pattern Recognition (CVPR)*, pages 3085–3094, 2019. [2](#)
- [83] Huajun Zhou, Xiaohua Xie, Jian-Huang Lai, Zixuan Chen, and Lingxiao Yang. Interactive two-stream decoder for accurate and fast saliency detection. In *IEEE Conference on Computer Vision and Pattern Recognition (CVPR)*, pages 9141–9150, 2020. [6](#)
- [84] Song Chun Zhu and David Mumford. Grade: Gibbs reaction and diffusion equations. In *IEEE International Conference on Computer Vision (ICCV)*, pages 847–854, 1998. [5](#)
- [85] Yuliang Zou, Zizhao Zhang, Han Zhang, Chun-Liang Li, Xiao Bian, Jia-Bin Huang, and Tomas Pfister. Pseudoseg: Designing pseudo labels for semantic segmentation. In *International Conference on Learning Representations (ICLR)*, 2020. [2](#)

6. Supplementary Materials

6.1. The base model performance

Tab. 2 (Complementary to Table. 2 of the paper) shows the average performances (including mean absolute errors M) and their corresponding standard deviations of the “Base”, the “NP” and our model “Full” trained with 1/16 data split ratio on the six benchmark testing datasets. These results are obtained by performing training 5 times for each model. Each training run adopts a different set of labeled data randomly selected from the DUTS training dataset with different random seeds (5 different labeled sets in total). It can be observed that our “Full” model outperforms both the “Base” and the “NP” on all six testing datasets with F-max nad mean absolute error measures, demonstrating the efficacy of our pseudo-label based learning framework as well as the importance of modelling a non-Gaussian distribution for the prior latent variable. The improvements are smaller in the mean absolute error measure than those in the F-max measure. This can be attributed to the fact that we use few fully-labeled samples and soft pseudo-labels on the unlabeled set to train the model. This results in our “Full” model making correct, although less binarised, prediction values.

7. Vary the labeled set (both the size and the samples)

Fig. 5 (Complementary to Figure. 4 in the paper) shows our baseline, FC-SOD [73] and our model trained with six data splits including 1/64, 1/32, 1/16, 1/8, 1/4 and 1/2 on the DUT-OMRON [69] and SOD [38] testing datasets. It can be seen that the performance of our baseline trained with only labeled data increases with an expanding labeled set. It demonstrates a similar trend to the performance of FC-SOD as the labeled set ratio increases from 1/64 to 1/2. Although the performance of FC-SOD does not plateau in DUT-OMRON when the labeled set ratio is above 1/16, as in other testing datasets, our model still outperforms both our baseline and FC-SOD with all data split ratios on both testing datasets. The most significant improvements of our model over both baseline and FC-SOD are observed in low data regimes, *e.g.* 1/64 and 1/32. Our model trained with a 1/32 label ratio achieves similar performance to FC-SOD trained with a 1/2 label ratio on the DUT-OMRON dataset. On the SOD dataset, our model requires only 1/32 labeled data to perform similarly to FC-SOD trained with a 1/2 label ratio.

8. Alternative deterministic and generative semi-supervised solutions

Fig. 6 illustrates several popular semi-supervised learning methods, including (1) consistency regularisation, (b) pseudo-label, (3) GAN and (4) VAE, along with our solu-

tion. The Π model and Mean Teacher (MT), belonging to consistency regularisation based methods, are implemented as alternative deterministic models. Both GAN and VAE are implemented as alternative generative models that generate pseudo-labels and a confidence map on the unlabeled set.

8.1. Performance

Tab. 5 (Complementary to Table. 3 of the paper) compares the performances of alternative deterministic and generative semi-supervised solutions with our model. It demonstrates that our model (“Ours”) also outperforms both alternative deterministic and generative solutions on the mean absolute error measure.

8.2. Pseudo-label and confidence map of generative solutions

Fig. 7 shows more pseudo-labels and confidence maps of GAN, VAE and EBM (Ours) on the unlabeled set. It can be seen that our method produces higher-quality pseudo-labels that are associated with accurate confidence maps, highlighting its errors.

8.3. The Π Model Implementation

The Π Model [51] adopts a typical U-Net structure with a ResNet50 encoder and the decoder of MiDaS [49]. It enforces consistent predictions for training images under different data augmentation techniques. Each training image is forward propagated twice through the network under different combinations of scaling, rotation and flipping. The training is single-phase, involving both labeled and unlabeled images. The total loss is defined as $\mathcal{L} = \mathcal{L}_{sup} + \mathcal{L}_{con}$, where \mathcal{L}_{sup} is a binary cross-entropy loss on the labeled data and \mathcal{L}_{con} is an L2 loss applied to both labeled and unlabeled data.

8.4. Mean Teacher (MT) [54]

MT [54] has a teacher model and a student model, each adopting a U-Net structure with a ResNet encoder and the decoder of MiDaS [49]. The teacher model adopts the moving average of the weight of the student model as defined in

$$\theta_t^T = \alpha \theta_{t-1}^T + (1 - \alpha) \theta_t^S \quad (12)$$

where T and S indicate the teacher and the student model, t denotes the current training epoch and α is a hyperparameter that we empirically set to 0.95. Consistency is enforced between predictions of the teacher and the student model for each input image.

8.5. GAN

GAN has a pair of generator, f_θ , and discriminator, g_β , models. The generator model adopts a U-Net structure with

a ResNet50 encoder and the decoder of MiDaS [49]. It takes a training image and a latent variable as input, with the latter being drawn from a Gaussian distribution $\mathcal{N}(0, \mathbf{I})$. The discriminator is a fully convolutional network (FCN) consisting of five 3×3 convolutional layers, each followed by a leaky ReLU activation function. The discriminator takes the input image and its corresponding ground truth (GT)/prediction as input and outputs a dense score map discriminating GT from coarse predictions. The generator and the discriminator models play a Min-Max game as defined in Eq. 13

$$\min_{f_\theta} \max_{g_\beta} V(g_\beta, f_\theta) = E_{(x,y) \sim p_{data}(x,y)} [\log g_\beta(y|x)] + E_{z \sim p(z)} [\log(1 - g_\beta(f_\theta(x, z)))], \quad (13)$$

$p_{data}(x, y)$ is the joint distribution of training data, $p(z)$ is the prior distribution of the latent variable z , which is usually defined as $p(z) = \mathcal{N}(0, \mathbf{I})$. In practice, we define the loss function for the generator as the sum of a binary cross-entropy loss \mathcal{L}_{ce} , and an adversarial loss $\mathcal{L}_{adv} = \mathcal{L}_{ce}(g_\beta(f_\theta(x, z)), 1)$, which is $\mathcal{L}_{gen} = \mathcal{L}_{ce} + \lambda \mathcal{L}_{adv}$, where the hyper-parameter λ is tuned, and empirically we set $\lambda = 0.1$ for stable training. \mathcal{L}_{ce} is the binary cross-entropy loss. The discriminator g_β is trained via loss function as: $\mathcal{L}_{dis} = \mathcal{L}_{ce}(g_\beta(f_\theta(x, z)), 0) + \mathcal{L}_{ce}(g_\beta(y), 1)$.

8.6. VAE

We implement a conditional variational auto-encoder (CVAE) [53] that includes includes 3 variables, namely the input image x , ground truth y and a latent variable z . The prior latent variable z from a Gaussian distribution is modulated by the input image x to generate the prediction y . There are two main models are included in the ‘‘VAE*’’, namely (1) a generator model $f_\theta(x, z)$ and (2) an inference model $q_\theta(z|x, y)$. Learning a CVAE framework involves approximation of the true posterior distribution of z with an inference model $q_\theta(z|x, y)$, with the loss function as:

$$\mathcal{L}_{cvae} = \underbrace{\mathbb{E}_{z \sim q_\theta(z|x, y)} [-\log p_\theta(y|x, z)]}_{\mathcal{L}_{rec}} + D_{KL}(q_\theta(z|x, y) \parallel p_\theta(z|x)), \quad (14)$$

where the first term is the reconstruction loss and the second is the Kullback-Leibler Divergence of prior distribution $p_\theta(z|x)$ and posterior distribution $q_\theta(z|x, y)$.

We have identical prior and posterior models in ‘‘VAE*’’ except the input layer, where the prior model takes an input image x and the posterior model takes the concatenation of an input image x and a latent variable z . There are in total five 4×4 convolutional layers, each followed by a batch normalisation layer and a ReLU activation layer, in each model. Two fully-connected layers are appended to map the feature map to vectors representing the mean μ and standard

deviation σ of the distribution of the latent variable z , which can be obtained as $z = \mu + \sigma \times \epsilon$ where $\epsilon \sim \mathcal{N}(0, \mathbf{1})$.

Table 4. Model performance (F_{ξ}^{\max}) w.r.t. the usage of unlabeled set (“Base” vs “Full”) and the prior distribution (“NP” vs “Full”).

Model	DUTS-TE [57]		DUT-OMRON [69]		PASCAL-S [68]	
	$F_{\xi}^{\max} \uparrow$	$\mathcal{M} \downarrow$	$F_{\xi}^{\max} \uparrow$	$\mathcal{M} \downarrow$	$F_{\xi}^{\max} \uparrow$	$\mathcal{M} \downarrow$
Base	0.840 ± 0.011	0.052 ± 0.004	0.748 ± 0.006	0.078 ± 0.007	0.846 ± 0.006	0.077 ± 0.004
NP	0.861 ± 0.006	0.050 ± 0.004	0.764 ± 0.005	0.076 ± 0.007	0.861 ± 0.005	0.072 ± 0.004
Full	0.869 ± 0.004	0.049 ± 0.004	0.774 ± 0.005	0.075 ± 0.007	0.864 ± 0.004	0.072 ± 0.004

Model	SOD [38]		ECSSD [52]		HKU-IS [31]	
	$F_{\xi}^{\max} \uparrow$	$\mathcal{M} \downarrow$	$F_{\xi}^{\max} \uparrow$	$\mathcal{M} \downarrow$	$F_{\xi}^{\max} \uparrow$	$\mathcal{M} \downarrow$
Base	0.840 ± 0.007	0.111 ± 0.004	0.919 ± 0.004	0.048 ± 0.001	0.915 ± 0.003	0.037 ± 0.001
NP	0.849 ± 0.006	0.109 ± 0.004	0.926 ± 0.002	0.046 ± 0.002	0.924 ± 0.001	0.035 ± 0.002
Full	0.856 ± 0.004	0.107 ± 0.003	0.931 ± 0.001	0.045 ± 0.002	0.928 ± 0.001	0.034 ± 0.001

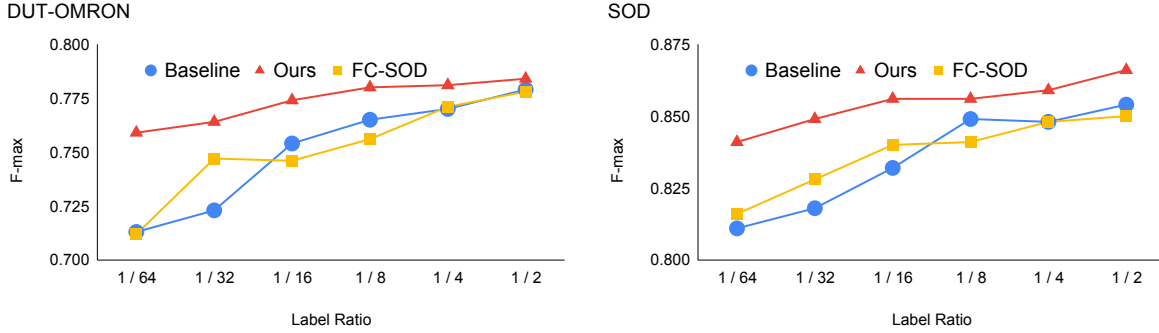


Figure 5. Comparisons of baseline, our model and FC-SOD trained on dataset splits including 1/64, 1/32, 1/16, 1/8, 1/4 and 1/2 on the DUT-OMRON and SOD datasets.

Table 5. Performance comparison between our model and the alternative deterministic and generative model based semi-supervised solutions on the benchmark testing datasets. * indicates our re-implementation.

Model	DUTS-TE [57]		DUT-OMRON [69]		PASCAL-S [68]		SOD [38]		ECSSD [52]		HKU-IS [31]	
	$F_{\xi}^{\max} \uparrow$	$\mathcal{M} \downarrow$										
Base*	0.840	0.058	0.748	0.090	0.850	0.075	0.829	0.125	0.917	0.052	0.911	0.043
II Model*	0.831	0.065	0.747	0.088	0.844	0.090	0.833	0.120	0.915	0.057	0.915	0.044
MT*	0.853	0.048	0.760	0.074	0.857	0.072	0.841	0.113	0.925	0.049	0.922	0.036
GAN*	0.852	0.046	0.761	0.069	0.855	0.071	0.836	0.116	0.925	0.048	0.920	0.035
VAE*	0.849	0.049	0.751	0.073	0.851	0.072	0.832	0.115	0.921	0.048	0.917	0.037
Ours	0.869	0.045	0.774	0.067	0.864	0.067	0.856	0.104	0.931	0.043	0.928	0.034

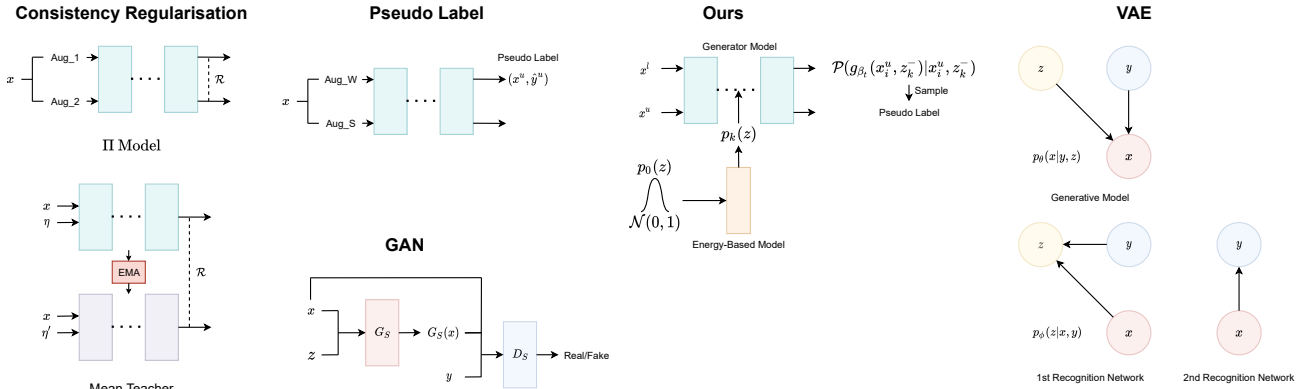


Figure 6. Illustrations of alternative deterministic and generative semi-supervised learning framework and our model. They can be categorised into (1) consistency-regularisation; (2) pseudo-label, (3) GAN and (4) VAE based methods.

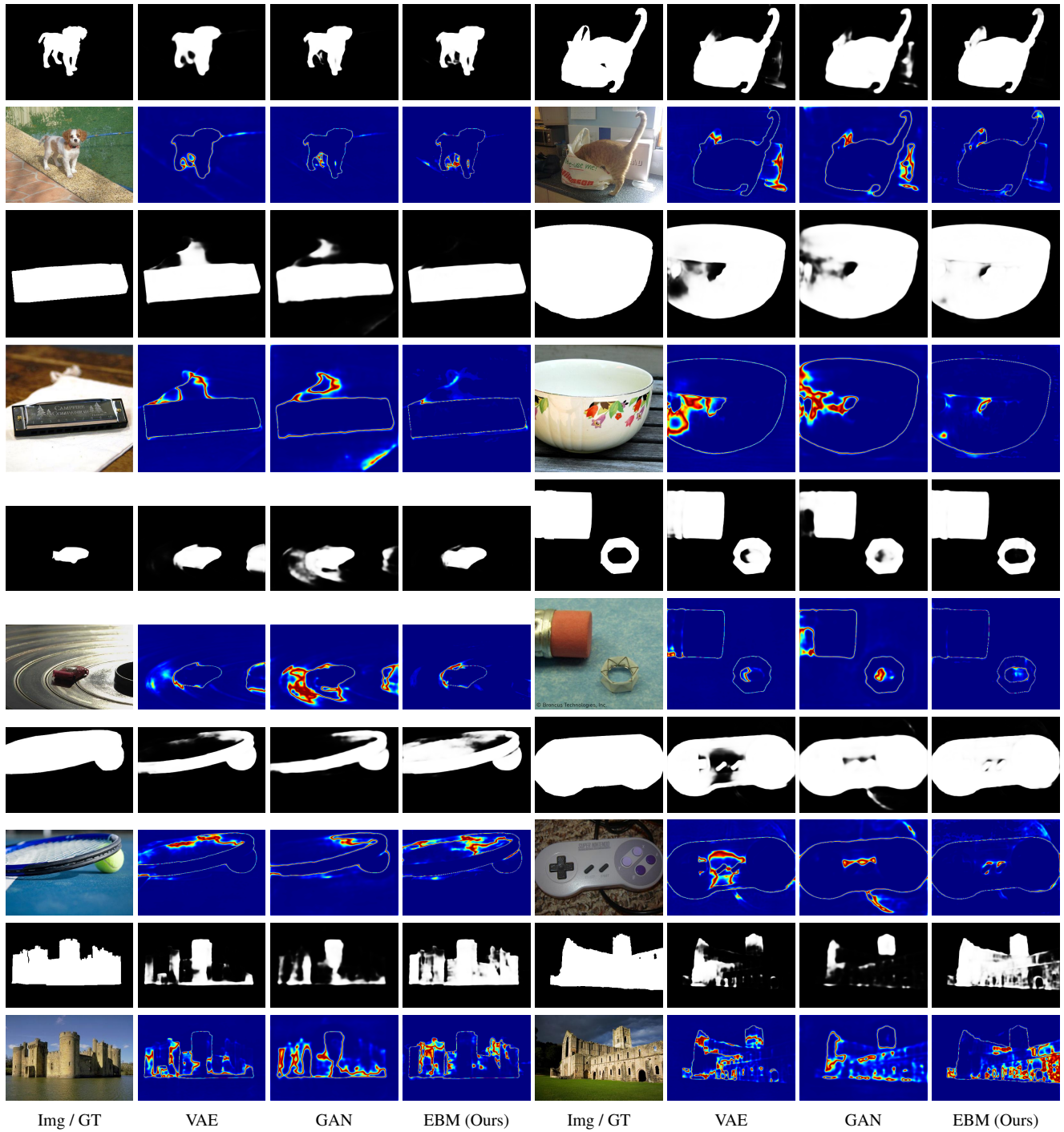


Figure 7. Pseudo-label and uncertainty map of the unlabeled training sample estimated by three generative models including VAE, GAN and EBM (Ours).